Advanced Powder Technology 27 (2016) 2291–2297

Contents lists available at ScienceDirect

Advanced Powder Technology

journal homepage: www.elsevier.com/locate/apt

Translated paper: SPTJ Best Paper Award 2015

Influence of anions on the structure and morphology of steel rust particles prepared by aerial oxidation of acidic Fe(II) solutions ☆

Hidekazu Tanaka [a,*], Nagisa Hatanaka [a], Miya Muguruma [a], Ayaka Nishitani [a], Tatsuo Ishikawa [b], Takenori Nakayama [c]

[a] Department of Chemistry, Graduate School of Science and Engineering, Shimane University, 1060 Nishikawatsu, Matsue, Shimane 690-8504, Japan
[b] School of Chemistry, Osaka University of Education, 4-698-1 Asahigaoka, Kashiwara, Osaka 582-8582, Japan
[c] Materials Research Laboratory, Kobe Steel, LTD., 5-5 Takatsukadai 1, Nishi-ku, Kobe, Hyogo 651-2271, Japan

ARTICLE INFO

Article history:
Received 30 August 2016
Accepted 2 September 2016
Available online 6 October 2016

Japanese version published in JSPTJ, Vol. 52 No. 1 (2015); English version for APT received on September 2, 2016.

Keywords:
Artificial steel rust
Atmospheric corrosion
Corrosive gas
Anion
Rust formation

ABSTRACT

In order to simulate the atmospheric corrosion of steel, artificial steel rust particles were synthesized by aerial oxidation of aqueous solutions containing $FeCl_2$, $FeSO_4$ and $NaNO_3$, and the structure and morphology of the obtained particles were characterized by XRD and TEM. Needle-like SO_4^{2-} containing Schwertmannite ($Fe_8O_8(OH)_6(SO_4)$) particles were mainly formed in $FeCl_2$–$FeSO_4$, $FeSO_4$–$NaNO_3$, $FeCl_2$–$FeSO_4$–$NaNO_3$ systems, and the crystallization and particle growth of this material were not influenced by added Cl^- and NO_3^-. The rod-shaped β-FeOOH particles were formed from in only $FeCl_3$-$NaNO_3$ system, though no marked change in crystallite and particle sizes of the β-FeOOH was recognized by adding NO_3^-. Accordingly, it can be suggested that the corrosive SO_X gas and air-borne chloride strongly affect the rust formation in atmospheric corrosion of the steels.

1. Introduction

The formation and structure of atmospheric corrosion products of steels strongly depend on the exposure environment of steels [1–3]. The air-borne chloride, SO_X and NO_X in atmosphere are dissolved in thin film water on the steels to generate anions such as Cl^-, SO_4^{2-} and NO_3^-, respectively. Then, Fe^{2+} is eluted from the steels and a part of Fe^{2+} is oxidized to Fe^{3+} by dissolved O_2. Therefore, the rust formation on the steel can regard as the reaction of Fe^{2+}, Fe^{3+} and anions in water. As a result, the α-FeOOH, γ-FeOOH and Fe_3O_4 rusts are mainly generated in atmosphere including NO_X and SO_X such as urban and industrial zones, while the β-FeOOH rust is formed in Cl^--containing environment such as marine zone including air-borne chloride [1–3]. Nevertheless, the detail role of anions on the formation of steel rusts is not fully established. To clarify this, several researchers have studied of this subject [4–8]. Ishikawa et al. and Kamimura et al. reported that the formation of β-FeOOH rust particles is suppressed by added SO_4^{2-}, while no significant effect of NO_3^- is seen [4,5]. Also, Sudakar et al. reported that the solubility of γ-FeOOH particles is increased by adding Cl^- and SO_4^{2-} [6]. Further, Oh et al. synthesized the steel rust particles from a mixture of $FeSO_4$ and $FeCl_2$ solutions and indicated that the existence of SO_4^{2-} enhances the α-FeOOH formation [7]. On the other hand, the authors studied the influence of Cl^-, SO_4^{2-} and NO_3^- on the formation of steel rust particles prepared from acidic Fe^{3+} solutions and indicated that added Cl^- accelerates the β-FeOOH formation and addition of SO_4^{2-} markedly inhibits the rust formation [8]. However, these studies are mainly discussed on the steel rust particles synthesized from Fe^{3+} solutions except for the study by Oh et al. [7]. In order to elucidate the atmospheric corrosion mechanism of steels at initial stage, systematic investigation about the influence of anions on the formation of steel rust particles prepared from Fe^{2+} solutions is more appropriate than that from Fe^{3+} solutions.

The purpose of this study was to clarify the influence of anions on the formation, structure and morphology of steel rust particles. So that, the artificial steel rust particles are synthesized by aerial oxidation of a mixture of aqueous $FeCl_2$, $FeSO_4$ and $NaNO_3$ solutions. The products thus prepared were characterized by means of powder X-ray diffraction and transmission electron microscope. The obtained results must serve to elucidate the role of air-borne chloride, SO_X and NO_X on the rust formation in atmospheric corrosion of steels.

☆ Open Access for this article was sponsored by the Society of Powder Technology, Japan, through the Grant-in-Aid for Publication of Scientific Research Results, Japan Society for the Promotion of Science, 2016.

* Corresponding author.
E-mail address: hidekazu@riko.shimane-u.ac.jp (H. Tanaka).

http://dx.doi.org/10.1016/j.apt.2016.09.004
0921-8831/

2. Experimental

2.1. Synthesis of steel rust particles

Artificial steel rust particles were prepared by aerial oxidation of acidic aqueous Fe^{2+} solutions in $FeCl_2$–$FeSO_4$, $FeCl_2$–$NaNO_3$, $FeSO_4$–$NaNO_3$ and $FeCl_2$–$FeSO_4$–$NaNO_3$ systems as follows. In $FeCl_2$–$FeSO_4$ system, 250 mL of a mixture of aqueous $FeCl_2$ and $FeSO_4$ solutions were prepared using deionized-distilled water. Then, the Fe^{2+} concentration was 1.0 mol/L and the molar ratio $X_{Cl} = FeCl_2/(FeCl_2 + FeSO_4)$ ranged from 0 to 1.0. In $FeCl_2$–$NaNO_3$, $FeSO_4$–$NaNO_3$ and $FeCl_2$–$FeSO_4$–$NaNO_3$ systems, desired amounts of $NaNO_3$ were added to 250 mL of 1.0 mol/L $FeCl_2$–$FeSO_4$ solution at molar ratio $NO_3^-/Fe(II) = 0$–1.0 and $X_{Cl} = 0$–1.0. Before the aging, pH of all the solutions was ca. 3.0. The solutions thus prepared were aged in a polypropylene vessel equipped with reflux condenser by aerial oxidation at 4 L/min and 50 °C for 24 h. The formed precipitates were filtered off using 0.45 μm Millipore filter, thoroughly washed with deionized-distilled water and finally dried at 50 °C for a over night. All the chemicals purchased from Wako Pure Chemical Industries Ltd., were used without further purification.

2.2. Characterization

The products thus formed were characterized by a variety of conventional techniques. Powder X-ray diffraction (XRD) patterns were taken on a Rigaku Miniflex-II diffractometer with a Ni-filtered Cu Kα radiation operated at 30 kV and 15 mA. The scanning speed and step were 2°/min and 0.01°, respectively. Morphology of the obtained particles was observed by a TOPCON EM-002B transmission electron microscope (TEM) at 200 kV.

3. Results and discussion

3.1. Yield of the products

Fig. 1 shows yield of the products in $FeCl_2$–$FeSO_4$, $FeCl_2$–$NaNO_3$, $FeSO_4$–$NaNO_3$, $FeCl_2$–$FeSO_4$–$NaNO_3$ systems. In $FeCl_2$–$FeSO_4$ system, yield of the products is 1.1 g at molar ratio $X_{Cl} = 0$ and is slightly decreased with the increase of X_{Cl}. In $FeSO_4$–$NaNO_3$ system, increasing $NO_3^-/Fe(II)$ ratio faintly increases yield of the products. On the other hand, no remarkable change in yield of the products is seen in $FeCl_2$–$NaNO_3$ system. In case of $FeCl_2$–$FeSO_4$–$NaNO_3$ system, yield of the products is increased with the decrease of X_{Cl} and the increase of $NO_3^-/Fe(II)$ ratio. These facts allow us to infer that adding SO_4^{2-} and NO_3^- accelerate the formation of steel rusts. The details of this will be discussed later.

3.2. Structure and morphology of rust particles formed in $FeCl_2$–$FeSO_4$, $FeSO_4$–$NaNO_3$ and $FeCl_2$–$NaNO_3$ systems

Fig. 2(A) shows the XRD patterns of the products formed in $FeCl_2$–$FeSO_4$ system at different X_{Cl}. At $X_{Cl} = 0$–0.75, the diffraction peaks characteristics of iron oxyhydroxysulfate named as Schwertmannite ($Fe_8O_8(OH)_6SO_4$) (PDF No. 47–1755) appear and the diffraction intensity is essentially unchanged by raising X_{Cl}. At $X_{Cl} = 1.0$, the Schwertmannite peaks disappear. Whereas, the β-FeOOH peaks (No. 34–1266) are developed in addition to Schwertmannite ones at $X_{Cl} = 0.75$ and are remarkably intensified at $X_{Cl} = 1.0$. The crystallite size of Schwertmannite estimated from the full width at half height of (2 1 2) peak using the Scherrer equation is almost constant of ca. 5 nm at $X_{Cl} = 0$–0.75. Fig. 2(B) displays the XRD patterns of the products yielded in $FeSO_4$–$NaNO_3$ system at $NO_3^-/Fe(II) = 0$–1.0. At $NO_3^-/Fe(II) = 0$–0.75, the diffraction peaks due to Schwertmannite mainly develop and no remarkable change in diffraction intensity and crystallite size of this material is seen by increasing $NO_3^-/Fe(II)$ ratio. Besides, new sharp peaks due to SO_4^{2-}-containing Natrojarosite ($NaFe_3(SO_4)_2(OH)_6$) (No. 51–1567) appear at $NO_3^-/Fe(II) \geqslant 0.50$. At $NO_3^-/Fe(II) = 1.0$, the intensity of Natrojarosite peaks is much larger than that of Schwertmannite ones, meaning that the major product turns to be Natrojarosite. Fig. 2(C) demonstrates the XRD patterns of the products formed in $FeCl_2$–$NaNO_3$ system at different $NO_3^-/Fe(II)$ ratios. At $NO_3^-/Fe(II) = 0$, all the peaks can be assignable to the β-FeOOH and the crystallite size evaluated from (3 1 0) peak is 45 nm. The diffraction intensity and crystallite size of this material are almost not changed by increasing $NO_3^-/Fe(II)$ ratio. Besides, the peaks related to secondary phase are not detected over the whole $NO_3^-/Fe(II)$ range.

Fig. 3 shows the TEM pictures of the particles obtained in $FeCl_2$–$FeSO_4$ system at various X_{Cl}. At $X_{Cl} = 0$, the needle-like Schwertmannite particles with a size of ca. 200 nm in length and ca. 20 nm in width are found. No marked changes in size and shape of the Schwertmannite particles are recognized by raising X_{Cl}. Whereas, the rod-shaped β-FeOOH particles with a size of ca. 120 nm in length and ca. 25 nm in width slightly appear in addition to the Schwertmannite ones at $X_{Cl} = 0.75$. At $X_{Cl} = 1.0$, the size of the β-FeOOH particles increases to ca. 150 nm (length) and ca. 30 nm (width), while the Schwertmannite particles disappear. These facts allow us to infer that added SO_4^{2-} inhibits the growth of β-FeOOH particles, though the addition of Cl^- has no significant effect on the growth of Schwertmannite particles. Fig. 4 shows the TEM pictures of the products generated in $FeSO_4$–$NaNO_3$ system at different $NO_3^-/Fe(II)$ ratios. At $NO_3^-/Fe(II) = 0$–0.75, the needle-like Schwertmannite particles with a size of ca. 200 nm in length and ca. 20 nm in width are observed and the morphology of the particles is almost unchanged by increasing the $NO_3^-/Fe(II)$ ratio.

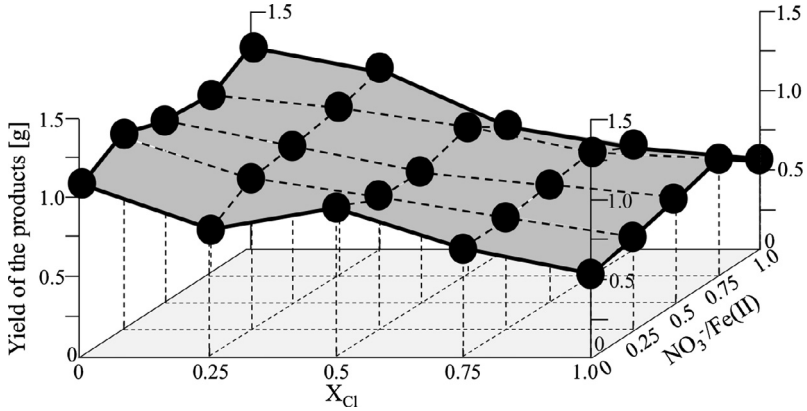

Fig. 1. Yield of the products formed in $FeCl_2$–$FeSO_4$–$NaNO_3$ system.